Fish and Shellfish Immunology 84 (2019) 1030–1040

Contents lists available at ScienceDirect

Fish and Shellfish Immunology

journal homepage: www.elsevier.com/locate/fsi

Full length article

Stress-immune responses and DNA protection function of thioredoxin domain containing 12 in zebrafish (*Danio rerio*)

D.C.M. Kulatunga[a], S.H.S. Dananjaya[a], Chamilani Nikapitiya[b,d], G.I. Godahewa[b], Jongki Cho[a], Cheol-Hee Kim[c], Jehee Lee[b,d], Mahanama De Zoysa[a,d,*]

[a] College of Veterinary Medicine, Chungnam National University, Yuseong-gu, Daejeon, 34134, Republic of Korea
[b] Department of Marine Life Sciences, School of Marine Biomedical Sciences, Jeju National University, Jeju Self-Governing Province, 63243, Republic of Korea
[c] Department of Biology, Chungnam National University, Yuseong-gu, Daejeon, 34134, Republic of Korea
[d] Fish Vaccine Research Center, Jeju National University, Jeju Self-Governing Province, 63243, Republic of Korea

ARTICLE INFO

Keywords:
Antioxidant
Immune defense
Oxidative stress
Thioredoxin domain containing 12
Zebrafish (*Danio rerio*)

ABSTRACT

Proteins with dithiol-disulfide oxidoreductase catalytic domain are well known for their capacity in the cellular redox homeostasis. In this study, we characterized the zebrafish thioredoxin domain containing 12 (Zf*txndc12*) gene, analyzed the transcriptional responses and studied the functional properties of its recombinant protein. Full-length cDNA of Zf*txndc12* consists 519 bp coding region encoding 172 amino acids (AA) including the signal peptide. Highly consensus active motif (^{65}WCGAC^{69}) and probable ER retrieval motif (^{169}GDEL^{172}) were identified. Ubiquitous expression of Zf*txndc12* mRNA was observed from one cell to juvenile stage as well as different organs of adult zebrafish. Moreover, whole mount *in situ* hybridization (WISH) results showed a higher expression of Zf*txndc12* in primordial gills, central nerves system and eye. The tissue specific expression analysis (by qRT-PCR) also showed the highest expression in gills followed by brain in adult zebrafish. In larvae, up-regulated Zf*txndc12* mRNA expression upon exposure to H_2O_2, *Edwardsiella tarda* and *Saprolegnia parasitica* suggests that it may involve in both stress and immune responses. Moreover, transcriptional expression of Zf*txndc12* was up-regulated upon *Streptococcus iniae* challenge in gills of adult zebrafish. The recombinant ZfTxndc12 (rZfTxndc12) was overexpressed, purified and tested for its biological activities. Results revealed that rZfTxndc12 is able to reduce the DNA damage and detoxify the H_2O_2 toxicity in concentration dependent manner. Overall results suggest that Zf*txndc12* is important antioxidant and immune functional member of the host defense system in zebrafish.

1. Introduction

Cellular oxidative stress reflects the imbalance of the harmony between the reactive oxygen species (ROS) or reactive nitrogen species (RNS) and the ROS scavengers [1]. During the cellular metabolism, a number of ROS are generated such as superoxide anion ($\cdot O_2^-$), hydrogen peroxide (H_2O_2), hydroxyl radical (•OH). ROS are produced as a result of normal cell functions or derived from external sources. In oxidative stress, they can irreversibly damage cell membranes, organelles and nucleic acids which lead to detrimental cell fate [2,3]. On the other hand, it is well known that ROS play vital roles in cellular functions such as autophagy, immune function such as killing phagocytosed pathogens [4,5]. Therefore, maintaining the cellular oxidative stress at a minimum level is beneficial to the host. Many enzymes with antioxidant properties such as protein disulfide isomerases (PDI), superoxide dismutase (SOD), catalase (CAT), glutathione disulfide reductase (GSR), peroxiredoxin (PRDX) and thioredoxin (TXN) defend against oxidative stress [6].

The TXN-like superfamily is a large, diverse group of proteins consist with a number of disulfide containing proteins with characteristic TXN fold, which express ubiquitously in almost all living organisms [7]. TXN active site consists of two cysteine residues containing thiol (-SH) groups. TXNs are involved in protein folding, re-folding of impaired thiol groups and thiol-disulfide exchange by redox regulation in protein thiol residues. TXN-like superfamily proteins are occupied in many other cellular processes including regulation of gene expression, redox signaling, cell proliferation and cellular senescence [8].

The different TXN proteins have specific locations in the cells such as nucleus, mitochondria, golgi apparatus, and endoplasmic reticulum (ER). Thioredoxin domain containing protein 12 (TXNDC12) is an ER

* Corresponding author. College of Veterinary Medicine, Chungnam National University, Yuseong-gu, Daejeon, 34134, Republic of Korea.
E-mail address: mahanama@cnu.ac.kr (M. De Zoysa).

https://doi.org/10.1016/j.fsi.2018.10.052
Received 25 July 2018; Received in revised form 16 October 2018; Accepted 22 October 2018
Available online 23 October 2018

localized TXN found in human and other animals. TXNDC12 protein is thought to be involved in number of cellular activities such as regulation of transcription factors, re-folding of disulfide containing proteins in ER, and act against oxidative stresses [9–11]. TXNDC12 has been characterized in human (designated as ERP18, ERP19 and ERP16) [12,13] and several other animals including fish. Homologues proteins of TXNDC12 have been identified in *Mus spp*., *Rattus spp*., *Xenopus spp.*, and *Caenorhabditis elegans* [12] and marine fish species, such as *Epinephelus coioides* [11], *Oplegnathus fasciatus* [14] and *Sebastes schlegelii* [15]. The detail study on Txndc12 has not been reported in freshwater fish, thus, as best of our knowledge, this is the first study focusing on *txndc12* gene in zebrafish, which is a well-known research model.

In the present study, the Zf*txndc12* gene was *in silico* characterized. qRT-PCR based expression analysis was performed in different developmental stages and adult tissues. The whole mount *in situ* hybridization (WISH) was performed to confirm the localized expression of Zf*txndc12* in early larval stages of zebrafish. Also, we investigated the transcriptional regulation of Zf*txndc12* in larval and adult zebrafish upon immune challenge and oxidative stress. The recombinant protein of Z*fTxndc12* was purified and its biological activities were evaluated by insulin disulfide reduction, metal catalyzed oxidation (MCO)-DNA nicking and extracellular H_2O_2 scavenging assays.

2. Materials and methods

2.1. Molecular characterization of Zftxndc12 gene

The reference sequence for Zf*txndc1*2 mRNA (NM_001020824.1) was retrieved from NCBI. BioEdit v:7.0 was used to derive the coding sequences (CDS) of Zf*txndc12*. Conserved domains of the Zf*txndc12* sequence were identified using NCBI conserved domain tool analysis (https://www.ncbi.nlm.nih.gov/Structure/cdd/wrpsb.cgi). Amino acid (AA) sequence alignment was performed by EMBOSS-sixpack tool (http://www.ebi.ac.uk/Tools/st/emboss_sixpack/). The DISULFIND tool (http://disulfind.dsi.unifi.it/) was used to predict disulfide bonds between AAs. Several tools of the ExPASy: SIB Bioinformatics Resource Portal (http://www.expasy.org/) including PROSITE, Motif Scan and SignalP were used to characterize the protein sequence. Protein parameter analysis was performed using ProtParam tool in ExPASy (http://web.expasy.org/tools/protparam/). Theoretical isoelectric point (pI) and molecular weight (Mw) of ZfTxndc12 were calculated using Compute pI/Mw tool (http://web.expasy.org/compute_pi/). Conserved regions of ZfTxndc12 were determined by aligning other vertebrate sequences using the Clustal Omega tool (https://www.ebi.ac.uk/Tools/msa/clustalo/). The evolutionary relationship (phylogenetic analysis) of the gene among other vertebrates was explored by neighbor-joining (NJ) method based on ClustalW protein sequence alignment using MEGA 6.0 program. The bootstrap values were replicated 1000 times to obtain the confidence value for the analysis. Tertiary structures of ZfTxndc12 was simulated by the SWISS-MODEL server (http://swissmodel.expasy.org/) and visualized by PyMOL molecular graphic system.

2.2. Zebrafish rearing and maintenance

For all the experiments, fish were kept under standard maintaining conditions in the automated circulatory system [16]. The temperature at 28.5 °C and day-night (14 h light/10 h dark) cycles were maintained automatically. Fish were fed with commercial feed formulations and live feed (brine shrimp) for 3 times per day. Well grown and uniform sized adult zebrafish were selected for the experiments. Wild type zebrafish were provided by the Zebrafish Center for Disease Modeling (ZCDM), Republic of Korea. All experiments with zebrafish were conducted according to approved guidelines and regulations of the Animal Ethics Committee of Chungnam National University (CNU-00866).

2.3. Zebrafish embryo and tissue collection

The samples were collected at different developmental stages of zebrafish (0, 6, 12, 18, 24, 36, 48 hours post fertilization, hpf and 3, 4, 5, 6, 7, 15, 30, 60 days post fertilization,dpf). Number of embryos and larvae collected at each development stage are shown in Table S1. Well grown adult zebrafish were anesthetized using fish tank water containing 160 μg/mL of buffered tricaine (Ethyl 3-aminobenzoate methanesulphonate), and gill, brain, liver, spleen, kidney, muscle and digestive tract were collected for RNA isolation. All the stages of embryos, larvae and different tissues were snap-frozen in liquid nitrogen and stored at −80 °C until further use. Samples of embryonic and larval developmental stages were formalin fixed and stored in methanol as described previously [17] for WISH experiments. Embryos of > 18 hpf were incubated in 0.002% Phenylthiourea (PTU) containing egg water to prevent the pigmentation.

2.4. Oxidative stress and immune challenge

2.4.1. Larvae

The zebrafish larvae (5 dpf) were exposed to chemical (H_2O_2) and biological (bacteria and oomycete) stressors for 24 h at 28.5 °C. The larvae were exposed to non-lethal concentration of H_2O_2 (0.003%), bacteria *Edwardsiella tarda* (3×10^7 CFU/mL), and oomycete *Saprolegnia parasitica* (3×10^4 spores/mL). The control group (5 dpf larvae) was maintained under same conditions without any treatment. Then larvae were snap-frozen in liquid nitrogen at 24 h post exposure (hpe) and stored at −80 °C. All the treatments were carried out with 50 larvae per replicate.

2.4.2. Adult fish

Adult zebrafish (300 mg in body weight) were immune challenged with Gram positive bacteria (*S. iniae*) by injecting intraperitoneally (i.p.). Briefly tryptic soy broth (TSB) culture of *S. iniae* in exponential growth (OD_{600} = 0.25) was centrifuged at 3500 rpm and re-suspended in phosphate buffered saline (PBS) to adjust OD_{600} at 0.2. *Streptococus iniae* with the concentration of 1×10^6 CFU/fish was injected as 10 μL volumes into each fish and the same volume of PBS was injected as a control. Fish were anesthetized and dissected to isolate gill tissues at different time points (3, 24, 48 and 72 h post infection; hpi). Isolated tissues were snap-frozen in liquid nitrogen and stored at −80 °C until RNA extraction.

2.5. RNA extraction and cDNA synthesis

Total RNA was extracted from eggs, developmental stages of larvae and different tissues using TRIzol® reagent (Invitrogen, USA) according to the manufacturer's protocol. After measuring the RNA concentration using a spectrophotometer, the concentration of the RNA was adjusted to the 500 ng/μL using nuclease free water. The first strand cDNA was synthesized using 2.5 μg of total RNA by PrimeScript 1st strand cDNA Synthesis Kit (TaKaRa, Japan) according to manufacturer's protocol. Finally, the cDNA was diluted 40-fold and stored at −20 °C until further use.

2.6. Digoxigenin (DIG) labeled riboprobe synthesize and In situ hybridization

2.6.1. DIG-labeled riboprobe synthesize

The corresponding DNA sequence which was required to synthesize RNA probe was retrieved by simple PCR with cDNA using ExTaq DNA polymerase. The PCR amplicon was ligated in to pGEM T-easy vector system (Promega, USA) and transformed into *Escherichia coli* DH5α according to standard protocols. Recombinant pGEM-T Easy plasmid with Zf*txndc12* probe sequence was isolated from 5 mL of overnight grown, transformed *E. coli* DH5α liquid culture using AccuPrep®

Plasmid Mini Extraction Kit (Bioneer, Korea) following its user protocol. The isolated recombinant plasmid was digested separately in two different reaction tubes with NcoI and SpeI (TaKaRa, Japan). *In vitro* transcription (IVT) was carried out to synthesize DIG-labeled ribonucleotide probe using SP6/T7 Dig RNA labeling kit (Roche, Germany).

2.6.2. In situ hybridization

Expression pattern of Zf*txndc*12 mRNA in embryonic zebrafish was studied by WISH technique according to the protocol adapted by Thisse and Thisse [17].

2.7. Quantitative real-time PCR analysis

Transcriptional expression of Z*ftxndc12* and other selected genes was analyzed by qRT-PCR using a TaKaRa Thermal Cycler Dice TP 800 real time system using gene specific primers (Table S2). The qRT-PCR was performed using SYBR Premix Ex-Taq (Perfect Real Time) master mix (TaKaRa, Japan) in a total reaction volumes of 10 μL containing 4 μL of cDNA, 5 μL of 2 x TaKaRa Ex-Taq™ SYBR premix and 0.5 μL of each forward and reverse primer (10 μM). the efficiency of the qRT-PCR primers were checked by qRT-PCR using serially diluted cDNA, and following the equation $E = (10^{(-1/-\text{slope})} - 1)$ x 100%. The expression fold was determined by the $2^{-\Delta\Delta CT}$ method (Livak method) [18]. Zebrafish *β-actin* was used as the internal reference gene to normalize the C_T values. For the relative mRNA expression fold analysis, cDNA originated from different developmental stages from one cell to juvenile were used. For tissue distribution mRNA analysis, cDNA originated from different tissues of adult zebrafish were used, and the digestive tract the lowest expression fold was taken as the basal expression (fold-1). For the determination of the mRNA expression under oxidative or immune stress, cDNA from H_2O_2, *E. tarda* and *S. parasitica* challenged larvae and *S. iniae* challenged adult fish gill tissue were used. The cDNA of PBS treated fish was used as the control.

2.8. Over-expression and purification of recombinant protein

Initially, *in silico* restriction mapping was performed to identify the internal restriction sites. *Bam*HI and *Hin*DIII over hanged PCR primers were used to clone the ORF (438 bp) of Z*ftxndc12* gene (without signal peptide sequence). Both PCR product and the expression vector pMAL-c2X (New England Biolabs, USA) were digested with *Bam*HI and *Hin*d III (TaKaRa, Japan) and gel purified by Accuprep™ gel purification kit (Bioneer, Korea). Vector-insert ligation was performed at 16 °C for 30 min followed by the overnight incubation at 4 °C using the Mighty Mix DNA Ligation Kit (TaKaRa, Japan). The recombinant construct was transformed into *E. coli* DH5α competent cells. The precise recombinant plasmid (confirmed by colony-PCR and sequencing) was transformed in to *E. coli* BL21(DE3) competent cells (New England BioLabs, UK). The over expression and purification of ZfTxndc12 was performed by following the instructions of pMAL™ Protein Fusion and Purification System (New England Biolabs, USA). Concentration of the purified protein was determined by the Bradford assay (Bio-Rad, USA). The crude protein (before purification) and un-induced samples along with the purified protein were further analyzed on a 12% SDS-PAGE gel stained with 0.05% Coomassie blue R-250.

2.8.1. In vitro activity of recombinant protein

2.8.1.1. Insulin disulfide reduction assay. *In vitro* dithiol-disulfide oxidoreductase activity of the rZfTxndc12 was evaluated by insulin disulfide reduction assay according to the previously described technique [19]. Briefly, the reaction mixture containing 100 mM potassium phosphate buffer (pH 7.0), 2 mM EDTA and 0.6 mM dithiothreitol (DTT) was prepared. Then, 50 and 100 μg/mL of rZfTxndc12 was added to the mixture. To initiate the reaction, final concentration of 150 mM bovine insulin was added to the each mixture and incubated at 25 °C. Resulting turbidity (insulin B-chain) was measured ($OD_{650\ nm}$) at every 10 min by spectrophotometer. Reaction mixture with 100 μg/mL recombinant maltose binding protein (rMBP) was used as a control.

2.8.1.2. MCO -DNA nicking assay. The MCO mediated DNA damage was assessed for the rZfTxndc12 with slight modifications as previously described [20]. Each 100 μL of MCO reaction mixture contained 4 mM DTT, 30 μM $FeCl_3$ and different rZfTxndc12 concentrations (6.25–100 μg/mL). The reaction mixtures were incubated for 2 h at 37 °C prior to add 1 μg of pUC19 circular DNA and further incubated for 30 min at 37 °C after adding the pUC19. For the control reaction, rZfTxndc12 was replaced with 200 μg/mL purified rMBP. At the end of the incubation, the reaction mixtures were purified using PCR purification kit (Bioneer, Korea) and examined on a 1% agarose gel.

2.8.1.3. H_2O_2 scavenging assay. Cell viability assay was performed to determine the ROS scavenging ability of the rZfTxndc12 using THP-1; human monocytic cell line as previously described [14]. Briefly, the THP-1 cells were cultured in RPMI 1640 media containing 10% fetal bovine serum (FBS), 100 mg/mL streptomycin, and 100 U/mL penicillin in 5% CO_2 incubator at 37 °C. Cells (5×10^5/mL) were incubated at different concentrations (0, 25, 50 and 100 μg/mL) of rZfTxndc12 or 100 μg/mL of rMBP for 30 min in the presence of 1 mM DTT followed by incubation for 24 h after 400 μM H_2O_2 was added to provide the oxidative stress. Then the cells were allowed to react with 20 μL of 5 mg/mL MTT (3-(4,5-dimethylthiazol-2-yl)-2,5- diphenyl tetrazolium bromide) for 30 min. The formazan residues produced by viable cells were spectrophotometrically measured at $OD_{560\ nm}$ and the cell viability percentage was calculated relative to the control.

2.9. Statistical analysis

In each experiment, minimum three replicates were used. Results were expressed as means ± standard error of the mean (SEM). The difference between mean values were analyzed using analysis of variance (ANOVA) followed by Tukey test in Statistical Analysis System (SAS 9.2 Institute Inc. Cary, NC, USA). All statistical analyses of the H_2O_2 or immune challenge experiments were based on the comparisons between each gene with respect to their control and treated or challenged groups, and statistics were carried out by unpaired t-tests. P value < 0.05 was considered as significant level.

3. Results

3.1. Sequence characterization of Zftxndc12

Firstly we amplified the Z*ftxndc12* ORF using the cDNA of gill tissue and sequenced to confirm it. The ORF of the sequence result was matched with NCBI reference sequence (NM_001020824.1). The mature Z*ftxndc12* transcript was 2255 bp in length with a 35 bp 5′- untranslated region (UTR), a 170 bp 3′ UTR and a 519 bp ORF encoding a 172 AA polypeptide with a deduced Mw of 19 kDa and theoretical pI of 5.2 (Fig. 1). At the N-terminal of the protein, 27 AA signal peptide was identified. After the cleavage of signal peptide, the molecular weight of the functional protein was calculated as 16 kDa. The distinctive conserved Txn active motif (^{65}Trp-Cys-Gly-Ala-Cys^{69}/^{65}WCGAC^{69}) in this protein has low confidence for disulfide bonding and remains in reduced state. At the C- terminal of the protein, probable ER retrieval motif (^{169}GDEL^{172}) was observed. Computational prediction of subcellular localization revealed that ZfTxndc12 is localized in endoplasmic reticulum (ER). ZfTxndc12 has total number of 26 and 17 negatively (Asp + Glu) and positively (Arg + Lys) charged residues. Moreover, the estimated half-life was 30 h and computed instability index was 33.41, hence classified the protein as stable. At 3′ UTR region, the polyadenylation signal sequence (AATAAA), two RNA instability motif sequences (ATTTA) and a polyadenylation (poly-A tail)

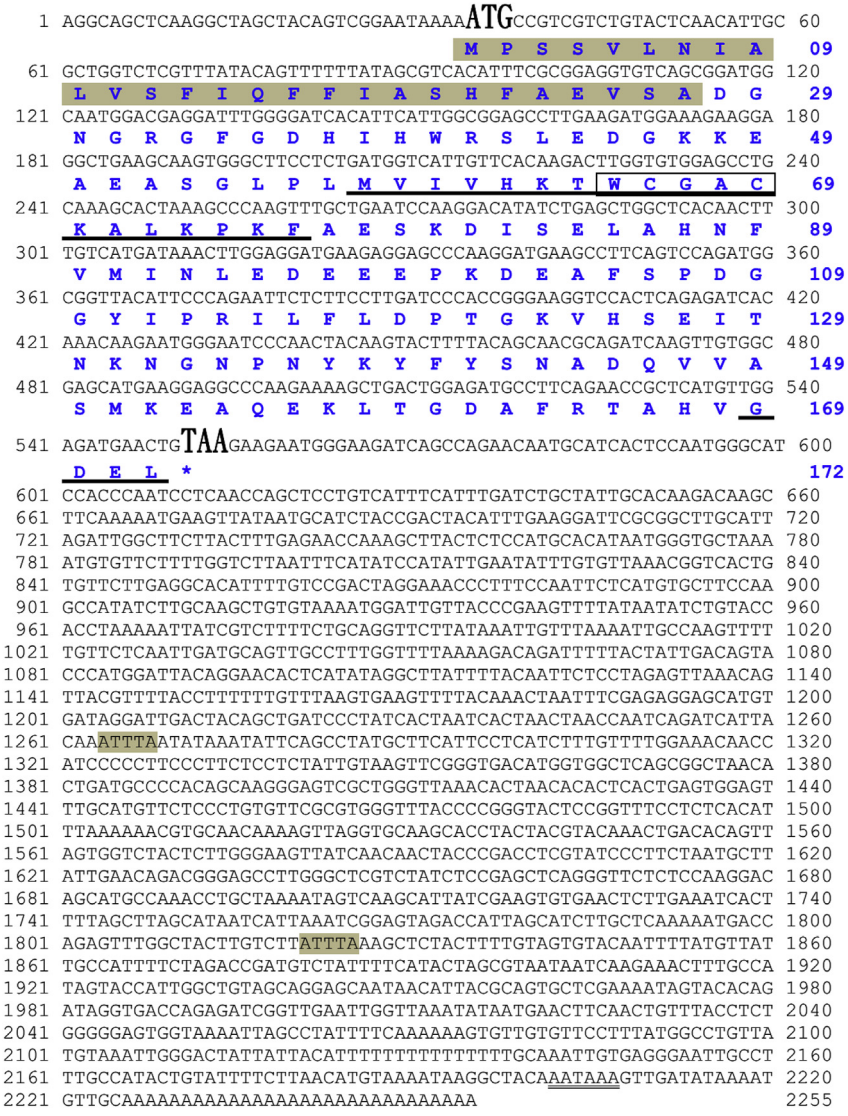

Fig. 1. Nucleotide and translated amino acid sequences of Zf*txndc12*. In the nucleotide sequence: start (ATG) and stop (TAA) codons are marked. Two mRNA destabilizing (ATTTA) sequences are shaded in gray. Poly adenylation signal sequence (AATAAA) is double underlined. In the amino acid sequence: N-terminal signal peptide is shaded in gray, thioredoxin family active site (^{58}M-F^{76}) and C- terminal ER retention sequence (^{169}GDEL^{172}) are underlined. The residues of conserved thioredoxin active motif (^{65}WCGAC^{69}) are underlined and boxed.

were identified. ClustalW Pair wise alignment analysis results showed highest identity to *O. mordax* (81.2%) followed by *S. salar* (80.2%) as listed in Table S3. ZfTxndc12 had 65.9% AA sequence identity to human TXNDC12. Multiple alignment of ZfTxndc12 AA sequence with vertebrate TXNDC12 counterparts showed higher sequence similarity (Fig. 2). Furthermore, Txn domain and conserved ZfTxndc12 active motif (WCGAC) were highly consensus and variation of AA length among different taxa was also minimized, ranging from 168 to 174 AA. The phylogenetic results indicated two major clades (Fig. 3). Members of TXNDC6 and TXNDC12 were grouped into one clade and on the other hand TXN1, TXN2, TMX1, PDI, PDIA5 and TXNDC5 have formed a separate clade. All the TXNDC12 sequences which represent invertebrates and vertebrates were grouped into a one clade. As expected ZfTxndc12 was closely grouped with teleost Txndc12 counterparts indicating the common ancestral origin. To predict the 3D structure of Zftxndc12, SWISS-MODEL template library [21] was used. The ZfTxndc12 structure had 81.38% sequence identity and 85% coverage with human TXNDC12 (PDB ID: 2k8v). In contrast, the predicted frog Txndc12 showed 86.13% sequence identity and 86% coverage with human TXNDC12. Moreover, comparison of predicted 3D structures of human, frog and zebrafish TXNDC12 displayed the high structural similarity in TXNDC12 active motif (Fig. 4).

3.2. Transcriptional responses of Zftxndc12 mRNA in zebrafish

3.2.1. Zftxndc12 mRNA expression at different developmental stages of zebrafish

The mRNA expression of Zf*txndc12* at different developmental stages were investigated to understand the growth specific expression profile by qRT-PCR (Fig. 5A) and WISH (Fig. 5 B). The developmental stages were categorized into i) single cell/zygote (0 hpf); ii) embryonic (6, 12, 18, 24, 36 and 48 hpf); iii) larval (3, 4, 5, 6, 7 and 15 dpf) and iv) juvenile fish (30 and 60 dpf). Expression results clearly showed the ubiquitous expression of Zf*txndc12* in all four selected stages. The highest expression was observed in single cell/zygote. However, when compared to 6 hpf stage the relative expression folds were higher in the embryonic (48 hpf), larvae (3–5 dpf) and juvenile (60 dpf). As shown in Fig. 5 B, WISH analysis results further confirmed the ubiquitously expression of Zf*txndc12* with highly expressed localization in primordial gills (branchial arches), central nerves system and eye (retina).

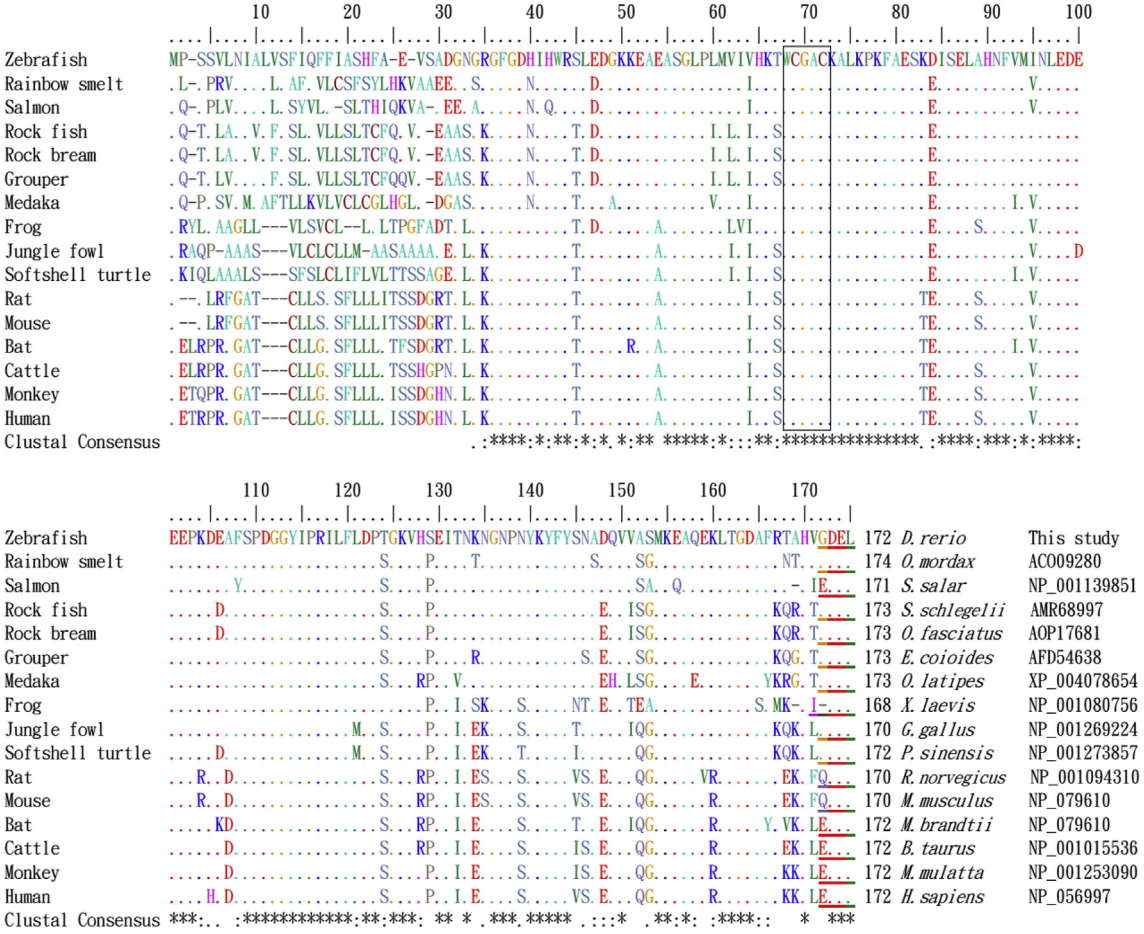

Fig. 2. Multiple alignment of ZfTxndc12 AA sequence with selected vertebrates TXNDC12 counterparts. Consensus TXNDC12 active motif (WCGAC) and C-terminal ER retention sequence (E/Q/I/GDEL) are boxed and underlined, respectively. Accession numbers, scientific names and AA sequence length are indicated at right side of each sequence.

3.2.2. Tissue specific expression of Zftxndc12 mRNA in adult zebrafish

To determine the tissue specific expression profile for Zf*txndc12* mRNA, qRT-PCR analysis was conducted using cDNA synthesized from different tissues with gene specific primers. The expression levels of each tissues were normalized to the expression levels of β-actin. The relative expression fold was compared with the expression fold of digestive tract which showed the lowest expression fold. Zf*txndc12* mRNA was constitutively expressed in all the investigated tissues in different levels (Fig. 6). Zf*txndc12* showed the highest expression in gills (19.3-fold) followed by brain (5.1-fold), liver (2.9-fold), spleen (2.2-fold), kidney (1.5-fold) and muscle (1.1-fold).

3.2.3. Transcriptional regulation of Zftxndc12 under H_2O_2 stresses and immune challenge

Transcriptional regulation of Zf*txndc12* was studied in zebrafish larvae under H_2O_2 exposure and *E. tarda* and *S. parasitica* immune challenge. Additionally, antioxidant transcription factor; nuclear factor erythroid 2–related factor 2 (Zf*nrf-2*) and several antioxidant genes including thioredoxin redicatase 1 (Zf*txnrd1*), catalase (Zf*cat*) and superoxide dismutase (Zf*sod*) were also investigated under the same experimental conditions. Expression of Zf*txndc12* and selected antioxidant genes (Zf*nrf-2*, Zf*txnrd1*, Zf*cat* and Zf*sod*) were up-regulated under H_2O_2 (Fig. 7A) and *E. tarda* (Fig. 7B) exposure compared to untreated control larvae. However, Zf*txndc12* was not highly induced by *S. parasitica* exposure while Zf*nrf-2* showed slightly higher expression (1.4-fold) compared to control (Fig. 7C). The basal or slight increment of the Zf*sod* and Zf*cat* mRNA expression levels were observed compared to control, nevertheless, higher individual variability was observed in Zf*nrf-2* and Zf*sod*, compared to other genes. Moreover, it was noticed that Zf*txndc12* and Zf*txnrd1* mRNA expressions were slightly down-regulated upon *S. parasitica* infection at 24 hpi.

3.2.4. Transcriptional responses of Zftxndc12 in adult zebrafish upon S. iniae infection

Zf*txndc12* gill mRNA expression in adult zebrafish after challenged with *S. iniae* at different post infection time points was gradually up regulated in adult zebrafish at 24 hpi (1.3-fold) and peaked (5.8-fold) at 72 hpi (Fig. 8).

3.3. Recombinant protein of ZfTxndc12 and its biological activities

3.3.1. Over-expression and purification of ZfTxndc12

rZfTxndc12 was over-expressed in *E. coli* BL21(DE3) and purified as a fusion of MBP using pMAL purification system. Level of induction, protein size and purity of rZfTxndc12 were determined by SDS-PAGE analysis (Fig. 9A). Strong protein band was observed in induced cells, crude protein/soluble protein fraction and purified rZfTxndc12 samples, but not in the same position of un-induced cells. Results clearly showed approximately 58.6 kDa strong band in purified sample which is in agreement with our predicted molecular mass 16.1 kDa (without signal peptide sequence), since the MBP has 42.5 kDa molecular mass (16.1 + 42.5 = 58.6 kDa).

3.3.2. Insulin disulfide reduction activity of ZfTxndc12

Activity of rZfTxndc12 mediated insulin disulfide reduction was determined in the presence of DTT (Fig. 9B). Highest reaction rate was

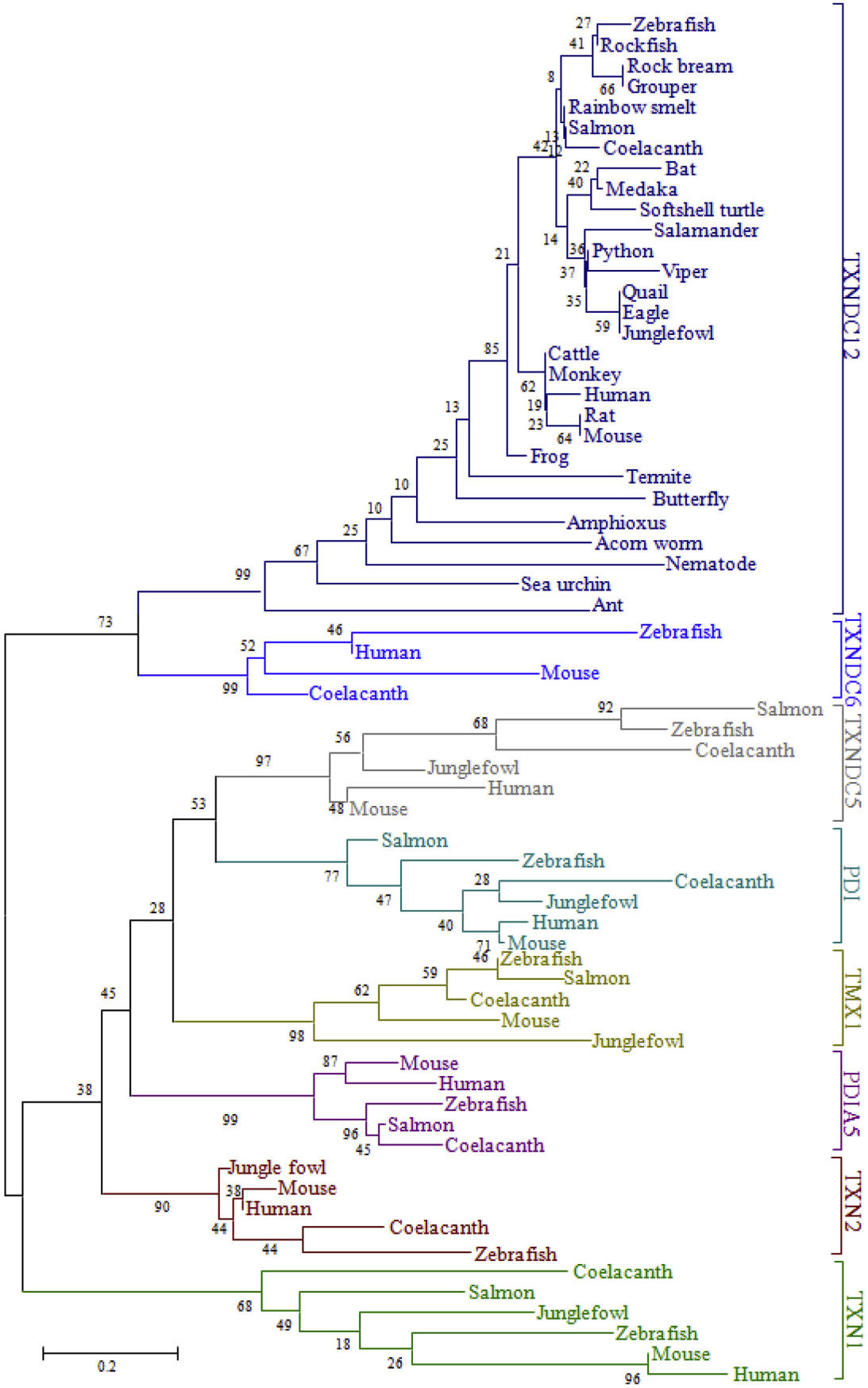

(caption on next page)

Fig. 3. Phylogenetic analysis of ZfTxndc12. The evolutionary relationship was determined by Neighbor joining method (NJ) based on ClustalW protein sequence alignment using MEGA 6.0 program. The numbers at the branches denote the bootstrap majority consensus values on 1000 replicates. GenBank accession numbers of sequences used for phylogenetic analysis are mentioned below. For TXNDC12, Human (*Homo sapiens*) AAH08913.1; Monkey (*Macaca mulatta)* NP_001253090.1; Cattle (*Bos taurus*) NP_001015536.1; Mouse (*Mus musculus*) NP_079610.1; Jungle fowl (*Gallus gallus*) NP_001269224.1; Quail (*Coturnix japonica*) XP_015726072.1; Eagle (*Aquila chrysaetos*) XP_011570534.1; Python (*Python bivittatus*) XP_007433010.1; Viper (*Protobothrops mucrosquamatus*) XP_015666390.1; Garden snake (*Thamnophis sirtalis*) XP_013925712.1; Salamander (*Ambystoma mexicanum*) AGG20200.1; Coelacanth (*Latimeria chalumnae*) XP_006005062.1; Salmon (*Salmo salar*) NP_001139851.1; Rainbow smelt (*Osmerus mordax*) ACO09280.1; Medaka (*Oryzias latipes*) XP_004078654.1; Rockfish (*Sebastes schlegelii*) AMR68997.1; Grouper (*Epinephelus coioides*) AFD54638.1; Rock bream (*Oplegnathus fasciatus*) AOP17681.1; Zebrafish (*Danio rerio*) NM_001020824.1; Termite (*Zootermopsis nevadensis*) KDR08987.1; Butterfly (*Danaus plexippus*) EHJ76926.1; Amphioxus (*Branchiostoma floridae*) XP_002602566.1; Acorn worm (*Saccoglossus kowalevskii*) XP_002739467.1; Nematode (*Caenorhabditis elegans*) NP_496599.1; Sea urchin (*Strongylocentrotus purpuratus*) XP_791682.2; Ant (*Trachymyrmex zeteki*) KYQ59836.1. For Txndc6, Human XP_016861795.1; Mouse NP_001159429.1; Coelacanth XP_014352867.1 and zebrafish NP_001082944.1. For Txn1 Human; NP_003320.2; Mouse NP_035790.1; Jungle fowl NP_990784.1; Coelacanth XP_005996498.1; Salmon XP_014065433.1 and Zebrafish NP_001002461.1. For Tmx1, Mouse NP_082615.1; Jungle fowl NP_001186337.1; Coelacanth XP_014343872.1; Salmon XP_014066986.1 and Zebrafish NP_001108605. For Txndc5, Human NP_110437.2; Mouse NP_663342.3; Jungle fowl XP_015131374.1; Coelacanth XP_006002933.1; Salmon XP_014015201.1 and Zebrafish; NP_998181.1. For Pdi, Human NP_000909.2; Mouse NP_035162.1; Jungle fowl NP_001185639.2; Coelacanth XP_005989098.1; Salmon XP_014032240.1 and Zebrafish NP_998529.3. For Pdia5, Human NP_006801.1; Mouse NP_082571.1; Coelacanth XP_014352855.1; Salmon NP_001133435.1 and Zebrafish NP_001107048.1. For Txn2, Human NP_036605.2; Mouse NP_064297.1; Jungle fowl NP_001026581.1; Coelacanth XP_006013272.2 and Zebrafish NP_991204.1.

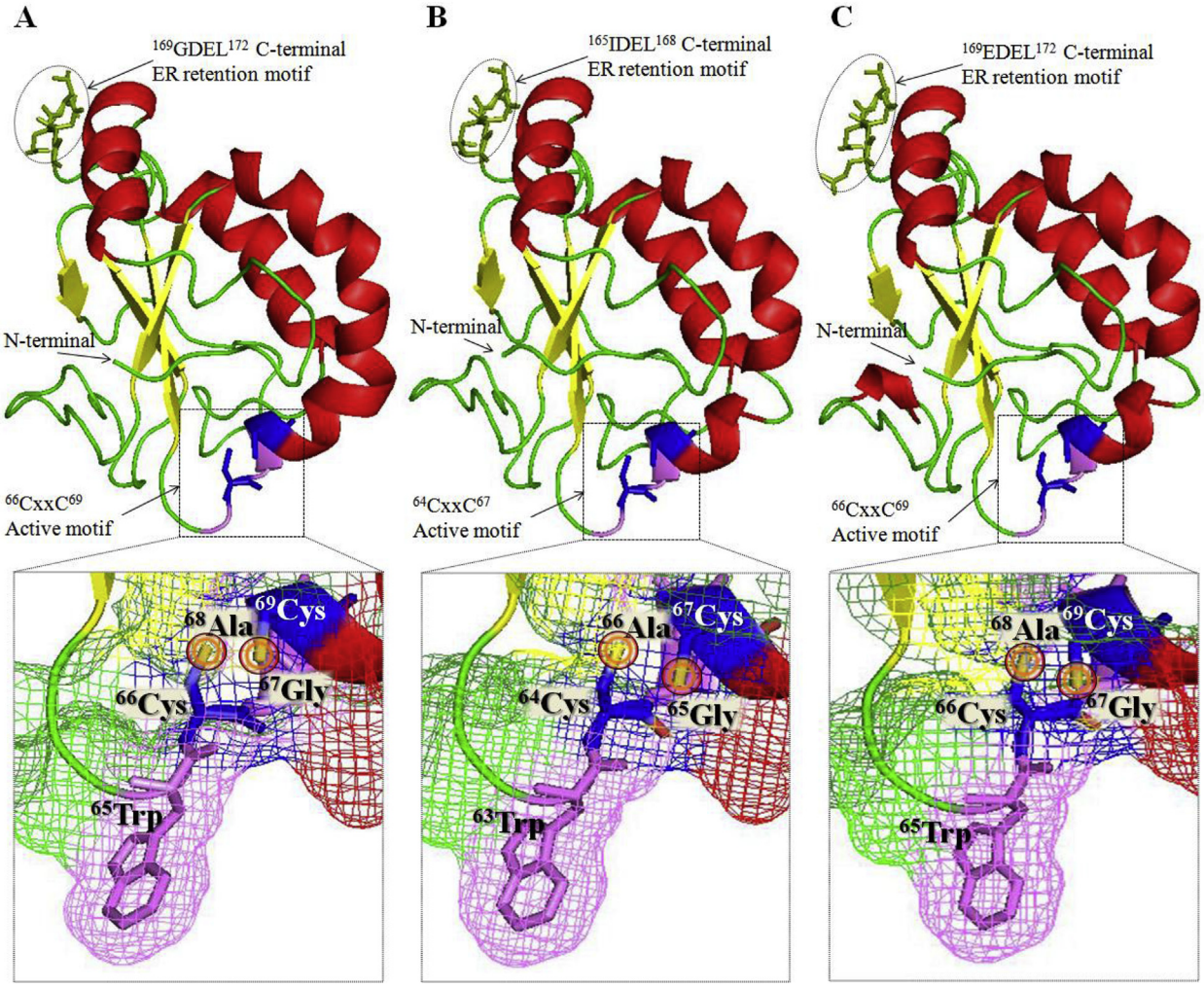

Fig. 4. Analysis of 3D structure of predicted ZfTxndc12 protein. Predicted 3D structures of zebrafish (A), frog (B) and human (C) were compared. Thioredoxin active site (CxxC) is squared. C-terminal ER retention motif is encircled in mature TXNDC12 protein (top). The magnified projection of squared site (bottom) displays the detailed atomic arrangement of the conserved active site including the thiol groups in the cysteine (Cys) residues (circled).

observed between 20 and 30 min of incubation with rZfTxndc12 (100 μg/mL), and the reaction was terminated at 60 min after the initiation. With the loweconcentration of rZfTxndc12, the rate of reaction was lower compared to that of high rZfTxndc12 concentration. Reaction mixtures without rZfTxndc12 and with rMBP showed almost zero reactivity with the insulin.

3.3.3. DNA protection activity of ZfTxndc12

Antioxidant activity of the purified rZfTxndc12 protein was studied by means of its DNA protection capacity against MCO system (Fig. 10A). When individual MCO system components incubated alone with pUC19, none of those components affected the circularity of the pUC19 (Fig. 10, lanes 1-3). However, incubation of pUC19 with the MCO system alone or MCO system with 200 μg/mL rMBP, showed

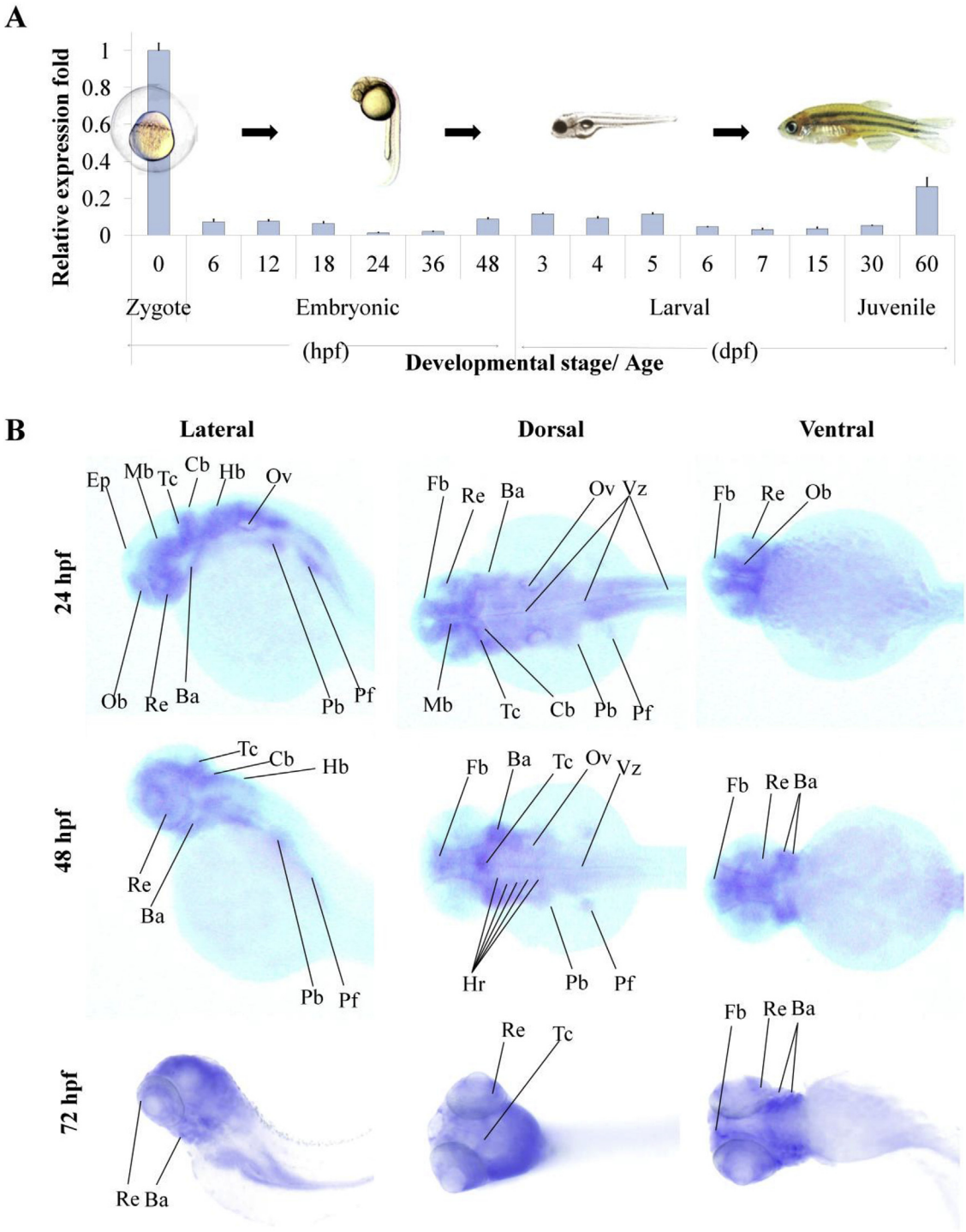

Fig. 5. Transcriptional expression of Z*ftxndc12* in developmental stages of zebrafish. A) The relative mRNA expression of Z*ftxndc12* in different developmental stages (zygote, embryonic, larval and juvenile) was analyzed by qRT-PCR. B) Spatiotemporal expression of Z*ftxndc12* in zebrafish embryos. WISH analysis of Z*ftxndc12* in zebrafish embryos at 24, 48 and 72 hpf. Highly expressed localizations were labeled as fore brain (Fb), retina (Re), branchial arch (Ba), hind brain (Hb), otic vesicle (Ov), ventricular zone (Vz), mid brain (Mb), posterior branchial arch (Pb), pectoral fin (Pf), epiphysis (Ep), olfactory bulb (Ob), tectum (Tc), cerebellum (Cb), and hindbrain rhombomeres (Hr).

totally degraded supercoiled DNA without a trace of nicked DNA on the gel profile (Fig. 10, lanes 4,5). With the increasing concentrations of rZfTxndc12 (6.25–200 μg/mL) in the MCO system, residual nicked (linearized) DNA was remained without further degrading (Fig. 10, lanes 6-11). At the higher rZfTxndc12 concentration, DNA protection property was further increased to keep some amount of circular pUC19 DNA under the MCO reaction (Fig. 10, lanes 9-11).

3.3.3.1. H_2O_2 scavenging activity of ZfTxndc12. To study the ROS scavenging properties of the rZfTxndc12, cell viability assay was performed under H_2O_2 driven oxidative stress (Fig. 10B). Compared to the control, cell viability was significantly reduced in all the oxidative stress induced reactions (T1 - T5). As we expected, the lowest cell viability was reported in the 500 μM H_2O_2 alone treated reaction mixture followed by 500 μM H_2O_2 + 100 μg/mL rMBP. However, the cell viability was significantly maintained at high level

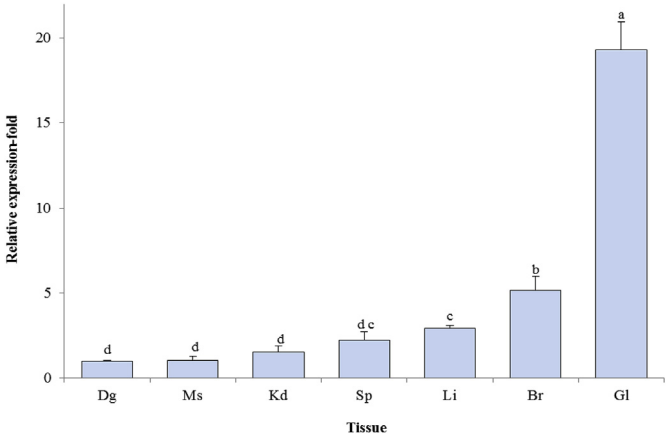

Fig. 6. Tissue-specific mRNA expression of Zf*txndc12* in adult zebrafish. The relative expression of Zf*txndc12* was carried out by qRT-PCR. Data are presented relative to that of digestive tract tissue. Tissues: digestive tract (Dg), muscle (Ms), kidney (Kd), spleen (Sp), liver (Li), brain (Br), gills (Gl). Differences were considered statistically significant at $p < 0.05$. Error bars represent the SEM ($n = 3$).

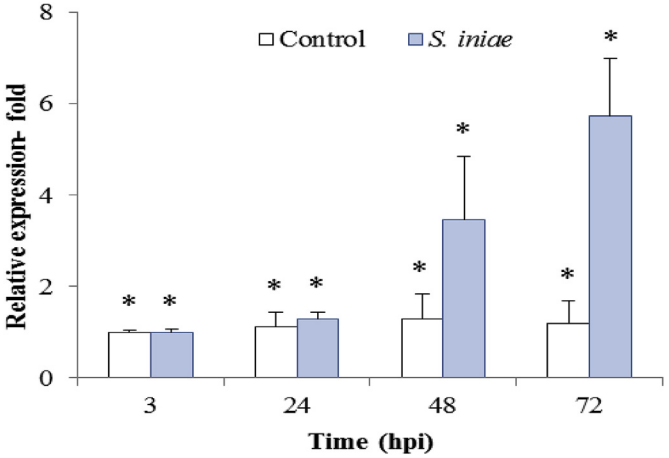

Fig. 8. Transcriptional responses of Zf*txndc12* in adult zebrafish upon *S. iniae* challenge. The relative expression fold was determined by qRT-PCR and presented relative to that of PBS-injected control group. Differences were considered statistically significant at $p < 0.05$. The data were represented as the means ± SEM (n = 3).

with the increasing concentrations of ZfTxndc12 protein compared to the H_2O_2 and rMBP treated samples.

4. Discussion

In this study, we describe the Zf*txndc12* as an important developmental and stress (oxidative and immune) responsive gene in zebrafish. ZfTxndc12 is a small (16.12 kDa) ER oxidoreductase protein involved in many cellular mechanisms. ZfTxndc12 shares characteristic features with the members of the Trx superfamily proteins. ZfTxndc12 compose of C-terminal ER retrieval GDEL motif which deviate from the common consensus ER retrieval motif; KDEL [12]. First residue of the ER retention motif of ZfTxndc12 was differed from most of the mammalian ER retention motif (Q/EDEL) and fish ER retention motif (EDEL) except rainbow smelt, and other members in PDI family. Though, EDEL differs from consensus ER retention motif, excellent ER localization nature has been shown previously [12]. Thus, it could assume that DEL would be the consensus residues which might contribute to its ER retention property.

Sequence similarity of thioredoxin domain of Txndc12 among different taxa has been previously described [11]. The characteristic active motif (^{65}Trp-Cys-Gly-Ala-Cys^{69}) produces unstable disulfide bonds similar to other Trx superfamily proteins [22]. However, it has low confidence for disulfide bonding and remains in reduced state. Reducing state is the active form of this protein, and it involves in disulfide isomerization in other native proteins [23,24]. This property of the protein is thought to be involved in redox regulation, repairing oxidized proteins and activation of transcription factors which involves several gene regulatory pathways [12].

The phylogenetic results demonstrate that the ZfTxndc12 is mainly clustered with fish counterparts and grouped with the fresh water teleost clade. Highly conserved multiple alignment results clearly showed that TXNDC12 is an evolutionary conserved protein among taxa. Generally, 3D structure of the protein reflects its functional properties [25], hence, structural similarity between human TXNDC12 and deduced ZfTxndc12 suggests the parallel role of both proteins among vertebrates.

In this study, we observed that Zf*txndc12* was expressed in all the developmental stages from zygote to juvenile fish in various levels. The highest expression level was at one cell stage, and it could be mainly due to the presence of maternal transcripts [26]. Early embryonic expression of Zf*txndc12* indicates the possible role in basic cellular activities during embryonic morphogenesis. Role of Txn on cell division and growth has been reported [27]. Furthermore, large-scale ISH screening [28] showed evidences for non-spatially restricted mRNA expression pattern of Zf*txndc12*. Moreover, a study with fish *O. fasciatus txndc12* also provides supportive evidences for systemic expression of this gene [14]. Similarly, the orthologous human gene is expressed ubiquitously including in the placenta [9], postulating the role of this gene since the human embryonic stage as well [10]. In this study, for

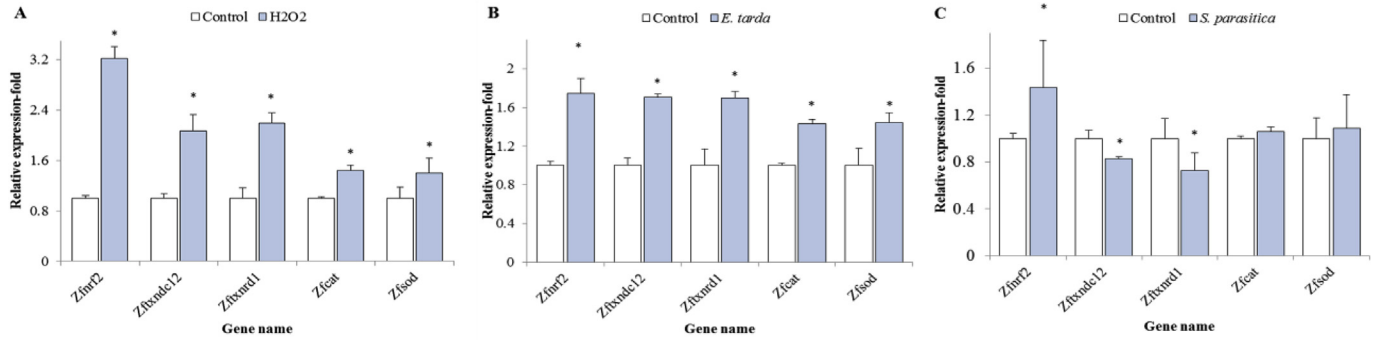

Fig. 7. Transcriptional regulation of Zf*txndc12* and selected antioxidant genes in H_2O_2, *E. tarda* and *S. parasitica* exposed zebrafish larvae. The expression level of Zf*txndc12*, Zf*nrf-2*, Zf*txnrd*, Zf*cat* and Zf*sod* were determined by qRT-PCR. A) H_2O_2 (0.003%); B) *E. tarda* (3×10^7 CFU/mL) and C) *S. parasitica* (3×10^4 spores/mL). Statistical analysis was based on comparisons between control and challenged groups. Differences were considered statistically significant at $p < 0.05$. The data was represented as the means ± SEM the standard error (n = 3).

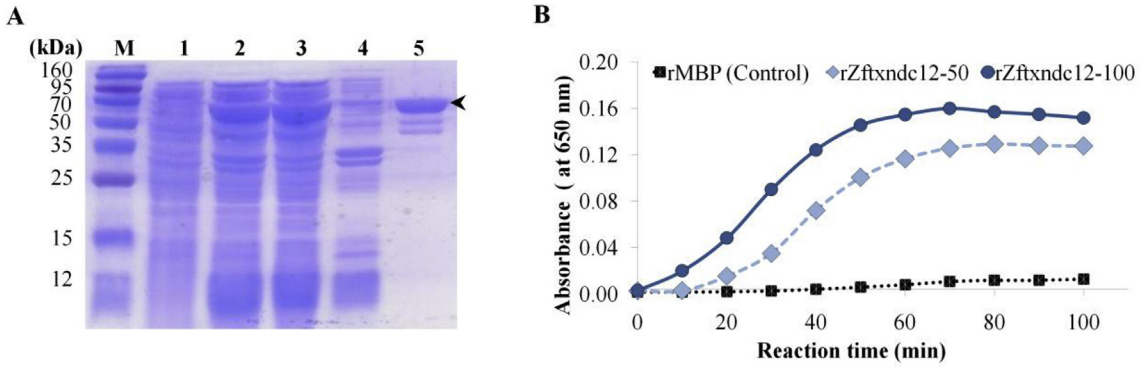

Fig. 9. Over expression, purification and antioxidant activity of rZfTxndc12 protein. A) SDS-PAGE analysis of the rZfTxndc12. M: Protein marker (TaKaRa, Japan); 1: Un-induced cellular extract; 2: induced cellular extract (total); 3: induced soluble/crude cellular extract (supernatant); 4: induced un-soluble pellet; 5: purified rZfTxndc12 (58.6 kDa) indicated by an arrow. **B)** *In vitro* insulin disulfide reduction activity of rZfTxndc12. rZfTxndc12-50: 50 μg/mL of rZfTxndc12; rZfTxndc12-100: 100 μg/mL rZfTxndc12; control: 100 μg/mL rMBP. Differences were considered statistically significant at $p < 0.05$. The data were represented as the means ± SEM (n = 3).

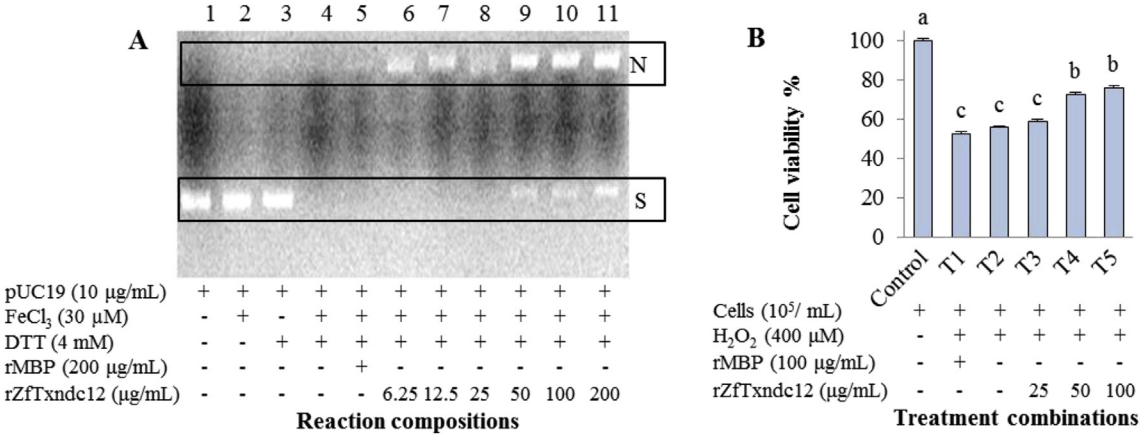

Fig. 10. DNA protection and *in vitro* ROS scavenging activity of rZfTxndc12. A) DNA protection activity of rZfTxndc12 by metal catalyzed oxidation/DNA nicking assay. Treatment of pUC19 plasmid with 1: circular pUC19; 2: pUC19 + $FeCl_3$; 3: pUC19 + DTT; 4: pUC19 + MCO system; 5: pUC19 + MCO system + rMBP (200 μg/mL); 6: pUC19 + MCO system + rZfTxndc12 (6.25 μg/mL); 7: pUC19 + MCO system + rZfTxndc12 (12.5 μg/mL); 8: pUC19 + MCO system + rZfTxndc12 (25 μg/mL); 9: pUC19 + MCO system + rZfTxndc12 (50 μg/mL); 10: pUC19 + MCO system + rZfTxndc12 (100 μg/mL); 11: pUC19 + MCO system + rZfTxndc12 (200 μg/mL); N: nicked pUC19 level and S: supercoiled pUC19 level on the gel. Supercoiled and nicked DNA traces after the MCO reaction are boxed with dotted line. B) H_2O_2 scavenging ability of rZfTxndc12 under H_2O_2 induced oxidative stress. H_2O_2 induced ROS scavenging ability of rZfTxndc12 was assayed by determining the cell viability percentage. ROS scavenging properties of rZfTxndc12 were studied by treating 400 μM H_2O_2 to THP-1 cells with different concentrations of rZfTxndc12 in the media. Treatment combinations are T1: 400 μM H_2O_2; T2: 400 μM H_2O_2 + 100 μg/mL rMBP; T3: 400 μM H_2O_2 + 25 μg/mL rZfTxndc12; T4: 400 μM H_2O_2 + 50 μg/mL rZfTxndc12; T5: 400 μM H_2O_2 + 100 μg/mL rZfTxndc12. The cells without any treatment were taken as a control. Cell viability was calculated as a percentage based on the control. The significant differences were analyzed by ANOVA followed by Tukey test ($p > 0.05$). Error bars represent the SEM (n = 3).

the first time, we demonstrate a high level of Zf*txndc12* expression in zebrafish embryonic and larval gills, eyes and CSN.

Generally, cells respond to oxidative stresses by expressing several antioxidant systems to re-establish the redox homeostasis [29–31]. The antioxidant response elements (AREs), usually found in promoter region of the antioxidant genes regulate the corresponding antioxidant gene expression via NRF-2 [32,33]. In response to oxidative stress, ROS cause nuclear translocation of NRF-2 to form a heterodimer with small MAF proteins in the nucleus. Then this complex interacts with ARE element and induces transcription of its target antioxidant genes [34–36]. Consequently, many antioxidant systems including Trx pathway are simultaneously up regulated via the NRF-2/ARE pathway in responses to oxidative stress. Induced expression of Zf*nrf-2* (also known as *nfe2l2b* in zebrafish) in larvae upon H_2O_2, *E. tarda* and *S. parasitica* challenge compared to controls suggests that induction of Zf*nrf-2* is important to activate antioxidant genes including Zf*txndc12* in zebrafish during pathogenic or oxidative stress in the host. Furthermore, we suggest that induction of Zf*txnrd1*, Zf*cat* and Zf*sod upon* H_2O_2 or bacteria exposure to zebrafish larvae could be mainly due to the regulatory function of Zf*nrf-2*. It could postulate that Zf*txndc12* is a ROS responsive (stress responsive) molecule, which could be regulated by Zf*nrf-2*. Although, Zf*nrf-2*, Zf*cat* and Zf*sod* were up-regulated by the fungal infection, down-regulation of Zf*txndc12* and Zf*txnrd1* was observed. This indicates that there might be some blockage of interaction of *nrf-2* with ARE element in those genes, or other mechanism might be involved against the fungi infection, which have not been studied yet. Although, thioredoxins are involved in cellular oxidative reactions, its immune role is not well understood. Up regulation of *txndc12* has been described in adult marine fish against bacterial and virus pathogens. For instance, upon bacterial challenge, *O. fasciatus* (Rock bream) *txndc12* was up regulated by 6-fold at 12 hpi [14], whereas, *txndc12* expression was highly up regulated at 24 hpi in *E. coioides* (Orange-spotted grouper) after challenge with sea-bream iridovirus [11]. With consistence to this, i.p. challenge with Gram positive *S. iniae*, Zf*txndc12* was induced in gills of zebrafish from 24 hpi, with the highest expression at 72 hpi and it gives further evidence for the immune

responsive role of Zf*txndc12*. In tissue distribution analysis, the highest Zf*txndc1*2 mRNA expression was observed in gills and therefore, gill tissue was selected to analyze the transcriptional regulation against *S. iniae*.

To investigate the biological activities, rZfTxndc12 protein (16.1 kDa) was over-expressed and purified as a fusion protein with MBP (42.5 kDa). Consistent with this, recombinant Txndc12 proteins of *E. coioides, S. schlegelii* and *O. fasciatus* also have shown similar molecular weights ranging from 15.9 to 16 kDa [11,14,15]. rZfTxndc12 displayed a potent disulfide reducing activity which has been reported in Txn family members [11,14]. It can be further confirmed that rZfTxndc12 carries a functional Txn active site to group it as a member of the Txn superfamily. Moreover, *in vitro* H_2O_2 scavenging activity results showed higher viability of rZfTxndc12 treated THP-1 cells under H_2O_2 oxidative stress. Therefore, it can be suggested that rZfTxndc12 protein has a an ability to protect the cells from H_2O_2 induced oxidative stress. The DNA protection activity of Txn family proteins have been described previously [37]. In the MCO system, Fe^{3+} reacts with DTT by generating ROS through the Fenton reaction [38]. Initially, free radicals produced by the Fenton reaction react with super-coiled, circular pUC19 plasmid forming DNA nicks. This this point, cleavage in the double strand linearizes the plasmid. Free radicals further react to degrade the cleaved DNA under continues reaction conditions. Purified rZfTxndc12 displayed a concentration dependent DNA protection activity against MCO system *in vitro* suggesting it may have higher activity under sub cellular environments.

5. Conclusion

In the present study, we have characterized the Zf*txndc12* gene, described its transcriptional responses, and further investigated the biological activities of its recombinant protein. The gene expression analysis revealed that Zf*txndc12* is a ubiquitous and fundamental gene which is being up-regulated according to the biotic and oxidative stresses. The disulfide reduction, DNA protection, and *in vitro* H_2O_2 scavenging activities of rZfTxndc12 conclude that ZfTxndc12 as a functional protein. Collectively, our findings indicated that Zf*txndc12* is a vital antioxidant and an immune gene for reducing harmful ROS during oxidative and pathogenic stress conditions.

Acknowledgement

This work was supported by the National Research Foundation of Korea grant funded by the Korea government (MSIP) (2018R1A2B6007841).

Appendix A. Supplementary data

Supplementary data to this article can be found online at https://doi.org/10.1016/j.fsi.2018.10.052.

References

[1] C. Gorrini, I.S. Harris, T.W. Mak, Modulation of oxidative stress as an anticancer strategy, Nat. Rev. Drug Discov. 12 (2013) 931–947.
[2] A. Barzilai, K.I. Yamamoto, DNA damage responses to oxidative stress, DNA Repair 3 (2004) 1109–1115.
[3] E. Panieri, M. Santoro, ROS homeostasis and metabolism: a dangerous liason in cancer cells, Cell Death Dis. 7 (2016) e2253.
[4] A.W. Segal, How neutrophils kill microbes, Annu. Rev. Immunol. 23 (2005) 197–223.
[5] J.M. Slauch, How does the oxidative burst of macrophages kill bacteria? still an open question, Mol. Microbiol. 80 (2012) 580–583.
[6] S.B. Nimse, D. Pal, Free radicals, natural antioxidants, and their reaction mechanisms, RSC Adv. 5 (2015) 27986–28006.
[7] J.J. Galligan, D.R. Petersen, The human protein disulfide isomerase gene family, Hum. Genom. 6 (2012) 1–15.
[8] K. Hirota, H. Nakamura, H. Masutani, J. Yodoi, Thioredoxin superfamily and thioredoxin-inducing agents, Ann. NY. Acad. Sci. 957 (2002) 189–199.
[9] W. Jeong, D.Y. Lee, S. Park, S.G. Rhee, ERp16, an endoplasmic reticulum-resident thiol-disulfide oxidoreductase: biochemical properties and role in apoptosis induced by endoplasmic reticulum stress, J. Biol. Chem. 283 (2008) 25557–25566.
[10] F. Liu, Y.P. Rong, L.C. Zeng, X. Zhang, Z.G. Han, Isolation and characterization of a novel human thioredoxin-like gene hTLP19 encoding a secretory protein, Gene 315 (2003) 71–78.
[11] J. Wei, H. Ji, M. Guo, Q. Qin, Isolation and characterization of a thioredoxin domain-containing protein 12 from orange-spotted grouper, *Epinephelus coioides*, Fish Shellfish Immunol. 33 (2012) 667–673.
[12] H.I. Alanen, R.A. Williamson, M.J. Howard, et al., Functional characterization of ERp18, a new endoplasmic reticulum-located thioredoxin superfamily member, J. Biol. Chem. 278 (2003) 28912–28920.
[13] M.L. Rowe, L.W. Ruddock, G. Kelly, J.M. Schmidt, R.A. Williamson, M.J. Howard, Solution structure and dynamics of ERp18, a small endoplasmic reticulum resident oxidoreductase, Biochemistry 48 (2009) 4596–4606.
[14] W.S. Thulasitha, Y. Kim, N. Umasuthan, R.G.P.T. Jayasooriya, G.Y. Kim, B.H. Nam, J. Lee, Thioredoxin domain-containing protein 12 from *Oplegnathus fasciatus*: molecular characterization, expression against immune stimuli, and biological activities related to oxidative stress, Fish Shellfish Immunol. 54 (2016) 11–21.
[15] W.S. Thulasitha, N. Umasuthan, R.G.P.T. Jayasooriya, J.K. Noh, H. Park, J. Lee, A thioredoxin domain-containing protein 12 from black rockfish *Sebastes schlegelii*: responses to immune challenges and protection from apoptosis against oxidative stress, Comp. Biochem. Physiol. C. 185–186 (2016) 29–37.
[16] M. Westerfield, A guide for the laboratory use of zebrafish (*Danio rerio*), in: M. Westerfield (Ed.), The Zebrafish Book, University of Oregon Press, Eugene, OR, 2007.
[17] C. Thisse, B. Thisse, High-resolution in situ hybridization to whole-mount zebrafish embryos, Nat. Protoc. 3 (2008) 59–69.
[18] K.J. Livak, T.D. Schmittgen, Analysis of relative gene expression data using real-time quantitative PCR and the $2^{-\Delta\Delta CT}$, Methods 25 (2001) 402–408.
[19] A. Holmgren, Thioredoxin catalyzes the reduction of insulin disulfides by dithiothreitol and dihydrolipoamide, J. Biol. Chem. 254 (1979) 9627–9632.
[20] Y.S. Lim, M.K. Cha, H.K. Kim, T.B. Uhm, J.W. Park, K. Kim, I.H. Kim, Removals of hydrogen peroxide and hydroxyl radical by thiol-specific antioxidant protein as a possible role in vivo, Biochem. Bioph. Res. Co. 192 (1993) 273–280.
[21] S.F. Altschul, T.L. Madden, A.A. Schaffer, J. Zhang, Z. Zhang, W. Miller, D.J. Lipman, Gapped BLAST and PSI-BLAST: a new generation of protein database search programs, Nucleic Acids Res. 25 (1997) 3389–3402.
[22] F. Aslund, K.D. Berndt, A. Holmgren, Redox potentials of glutaredoxins and other thiol-disulfide oxidoreductases of the thioredoxin superfamily determined by direct protein-protein redox equilibria, J. Biol. Chem. 272 (1997) 30780–30786.
[23] L. Ellgaard, L.W. Ruddock, The human protein disulphide isomerase family: substrate interactions and functional properties, EMBO Rep. 6 (2005) 28–32.
[24] B. Wilkinson, H.F. Gilbert, Protein disulfide isomerase, Biochim. Biophys. Acta 1699 (2004) 35–44.
[25] H.H. Gan, R.A. Perlow, S. Roy, et al., Analysis of protein sequence/structure similarity relationships, Biophys. J. 83 (2002) 2781–2791.
[26] L. Vesterlund, H. Jiao, P. Unneberg, O. Hovatta, J. Kere, The zebrafish transcriptome during early development, BMC Dev. Biol. 11 (2011) 1–18.
[27] J.R. Gasdaska, M. Berggren, G. Powis, Cell growth stimulation by the redox protein thioredoxin occurs by a novel helper mechanism, Cell Growth Differ. 6 (1995) 1643–1650.
[28] B. Thisse, V. Heyer, A. Lux, et al., Spatial and temporal expression of the zebrafish genome by large-scale in situ hybridization screening, Methods Cell Biol. 77 (2004) 505–519.
[29] A.R. Timme-Laragy, S.I. Karchner, D.G. Franks, rf2b, novel zebrafish paralog of oxidant-responsive transcription factor NF-E2-related factor 2 (NRF2), J. Biol. Chem. 287 (2012) 4609–4627.
[30] D.H. Kang, Oxidative stress, DNA damage, and breast cancer, AACN Clin. Issues 13 (2002) 540–549.
[31] C. Michiels, E. Minet, D. Mottet, M. Raes, Regulation of gene expression by oxygen: NF-kappaB and HIF-1, two extremes, Free Radical Bio. Med 33 (2002) 1231–1242.
[32] W.W. Wasserman, W.E. Fahl, Functional antioxidant responsive elements, P. Natl. Acad. Sci. USA 94 (1997) 5361–5366.
[33] S. Petri, S. Korner, M. Kiaei, Nrf2/ARE signaling pathway: key mediator in oxidative stress and potential therapeutic target in ALS, Neurol. Res. Int. 2012 (2012) 1–7.
[34] T. Ishii, K. Itoh, S. Takahashi, et al., Transcription factor Nrf2 coordinately regulates a group of oxidative stress-inducible genes in macrophages, J. Biol. Chem. 275 (2000) 16023–16029.
[35] Y. Katoh, K. Iida, M.I. Kang, et al., Evolutionary conserved N-terminal domain of Nrf2 is essential for the Keap1-mediated degradation of the protein by proteasome, Arch. Biochem. Biophys. 433 (2005) 342–350.
[36] J.M. Lee, J.A. Johnson, An important role of Nrf2-ARE pathway in the cellular defense mechanism, J. Biochem. Mol. Biol. 37 (2004) 139–143.
[37] M. De Zoysa, W.A. Pushpamali, I. Whang, S.J. Kim, J. Lee, Mitochondrial thioredoxin-2 from disk abalone (*Haliotis discus discus*): molecular characterization, tissue expression and DNA protection activity of its recombinant protein, Comp. Biochem. Physiol. B 149 (2008) 630–639.
[38] K. Kim, S.G. Rhee, E.R. Stadtman, Nonenzymatic cleavage of proteins by reactive oxygen species generated by dithiothreitol and iron, J. Biol. Chem. 260 (1985) 15394–15397.